DJS Vol. 49(1)(2024) – pp. 1-18 ISSN: 1012-5965

Delta Journal of Science

Available online at

https://djs.journals.ekb.eg/

Research Article

PHYSICS

Alpha elastically scattered by light nuclei using semi-microscopic and full-microscopic method

R. F. Madyan*, A. Amar and S. S. Saad

Physics Department, Faculty of Science, Tanta University, Tanta, Egypt

***Corresponding author:** R. F. Madyan **E-mail:** rowan151664@science.tanta.edu.

Received: 22/7/2024 **Accepted:** 4/9/2024

KEY WORDS

Double folding, Paulo São potential, alpha elastically scattered by ^{6,7}Li, ^{9}Be and ^{11}B

ABSTRACT

The present work aims to use semi-microscopic and full microscopic methods to analyze experimental data for alpha elastically scattered by ^{6,7}Li, ^{9}Be, and ^{11}B in the energy range from 26 to 166 MeV. In the semi-microscopic method, the double folding São Paulo Potential (SPP) was used as a real part of the optical potential, while the Woods-Saxon form was used as an imaginary part. In the present calculations, the real part of the optical potential is derived by folding the nucleon-nucleon (NN) interaction into the nuclear matter density distribution of the projectile and target nuclei using the computer code SPOMC3. The optical model parameters and the normalization factors have an influence on the fitting of the experimental data. The volume integral of the imaginary part of the optical potential and the cross-section were found to be energy-dependent. In the full-microscopic method, the SPP was used as both a real and an imaginary part.

Introduction

The study of alpha particle scattering on target nuclei like ^{6}Li, ^{7}Li, ^{9}Be, and ^{11}B using the double folding model represents a sophisticated approach to understanding nuclear interactions at a microscopic level. The double folding model, based on the effective nuclear interaction potential, offers a powerful tool for investigating the elastic scattering of alpha particles on various nuclei. This model considers the nuclear densities of both the projectile (alpha particle) and the target nuclei, along with the effective nucleon-nucleon interaction potential, to simulate the scattering process accurately. The folding model is one of the most widely used methods for determining the nucleus-nucleus interaction potential. There are many previous researches were studied alpha elastically scattered on light nuclei **(Qaim et al., 2016; Saad, 1995; Burtebaev et al., 2005; A. H. Amer et al., 2016; Burtebayev et al., 2020; Amar, 2022; Amer et al., 2021).** The elastic scattering of alpha particles by light nuclei has been studied using a double folding model that employs SPP as the real part of the optical potential. This model incorporates the concept of Pauli nonlocality, which accounts for the exchange of nucleons between the target nuclei and the projectile alpha particles. The choice of target nuclei, including ^{6}Li, ^{7}Li, ^{9}Be, and ^{11}B for alpha particle scattering studies using the double folding model is motivated by their unique nuclear properties and relevance in nuclear physics research. These nuclei exhibit distinct characteristics that make them ideal candidates for investigating the elastic scattering of alpha particles and extracting valuable information about nuclear structure and nuclear reaction mechanisms **(Alvarez et al., 2003; Chamon et al., 2002).** This work aims to investigate the differential cross-sections of alpha elastically scattered by light nuclei at low energies using semi-microscopic and full-microscopic models.

Theoretical Formalism

São Paulo potential (SPP)

SPP is a theoretical model used in nuclear physics to describe heavy-ion nuclear interaction. It has been successful in explaining various aspects of heavy-ion scattering, including elastic and inelastic interactions. The model was developed by a team of researchers at the University of São Paulo and has been widely used in the field of nuclear physics. The SPP is based on a double folding potential, which is a mathematical representation of the interaction between two nuclei. This

potential is calculated by folding the density distributions of the two nuclei with the nucleon-nucleon interaction. The model includes relativistic effects and is capable of describing the energy dependence of the optical potential, which is essential for understanding heavy-ion scattering. The SPP has been applied to a wide range of heavy-ion systems and has been shown to be effective in describing the elastic and inelastic scattering of various nuclei. It has also been used to study nuclear fusion and the properties of dense matter. The model continues to be an important tool in nuclear physics research, particularly in the study of heavy-ion interactions and nuclear reactions **(Chamon et al., 2002; Gómez et al., 2011; Ibraheem, 2016; Amer et al., 2021; Gasques et al., 2003; Ibraheem et al., 2020; Chamon 2007).** The SPOMC3 code **(Chamon, 2013)**was used to calculate the cross-section using double folding. It is based on SPP as the real part of the optical potential**.** The model has been used to calculate the total reaction cross-section **(Chamon, 2007; Amer et al., 2021).** In the semi-microscopic SM method, SPP was used as a real part of the optical potential whereas the imaginary part (W) was used Woods-Saxon form as:

$$\boldsymbol{V_{op} = N_R V_{SPP} + iW} \quad (1)$$

In the full microscopic FM method, SPP was taken as a real and imaginary part of optical potential as:

$$\boldsymbol{V_{op} = (N_R + iN_i) V_{SPP}} \quad (2)$$

Within this model, the nuclear interaction is connected with the folding potential through the relationship **(Chamon, 2007):**

$$\boldsymbol{V_{SPP}(r,E) = V_F(r) e^{-4v^2/c^2}}, \quad (3)$$

Where v is the local relative velocity between the interacting nuclei and c is the speed of light. The velocity dependence results from the effects of the Pauli non-locality, which comes from nucleon exchange between the alpha and the target. The relative velocity is given by **(Chamon, 2007)**:

$$\boldsymbol{v^2(r,E) = \frac{2}{\mu}[E - V_C(r) - V_{SPP}(r,E)]} \quad (4)$$

The velocity v related with the kinetic energy E_k is given by **(Chamon et al., 2002)** :

$$\boldsymbol{v^2(r,E)/c^2 = \frac{2}{\mu c^2} E_K(r)} \quad (5)$$

where μ represents the reduced mass of the system. The SPP is obtained numerically from solving Eqs. (1) and (2) by an iterative process. The folding potential $V_F(r)$ is calculated according to the relationship **(Alvarez et al., 2003) :**

$$V_F(r) = \int \rho_p(r_p)\,\rho_t(r_t) V_0 \delta\left(\left|\vec{r} + \vec{r_t} - \vec{r_p}\right|\right) d^3r_p d^3r_t. \quad (6)$$

Where $V_0 = -456$ MeV.fm^3, ρ_p and ρ_t are the nuclear matter densities of the projectile and the target nuclei, respectively. The densities of the targets are expressed in the form of a two-parameter Fermi (2pF) distribution as:

$$\rho(r) = \frac{\rho_0(C,M)}{1+\exp\left(\frac{r-R_0(C,M)}{a(C,M)}\right)} \quad (7)$$

Where $R_{0C} = (1.76\,Z^{1/3} - 0.96)$ fm and $R_{0M} = (1.31\,A^{1/3} - 0.84)$ fm represent the radii of charge and matter densities, respectively. a_c=0.53 fm and a_M=0.56 fm represent the average diffuseness values for the charge and matter density distributions of the target nuclei, respectively **(Chamon, 2007)**. The matter density distribution of ^{4}He is taken in the form of the Gaussian shape **(Amer et al., 2020):**

$$\rho_\alpha(r) = \rho_o \exp(-\beta r^2) \quad (8)$$

With ($\rho_o = 0.4229 fm^3$, β=0.7024) for α particles.

Results and Discussions

Alpha elastically scattered by ^{6}Li

Optical parameters of protons, deuterons, and alpha elastic scattering by ^{6}Li have particular significance in astrophysical studies. ^{6}Li is a weakly bound nucleus and has two configurations, ^{3}He+^{3}H and d+α **(Amar et al., 2022).** Thus, for obtaining the information of the ^{6}Li configuration, alpha is used as a projectile. In our study, we compared the experimental data and the theoretical predictions for Alpha elastically scattered on ^{6}Li at the 29.4, 50.5, 59.0, 104.0, and 166.0MeV energies are shown in Fig. (1). The potential parameters have been modified to reproduce differential cross-sections which are listed in Table (1). In the semi-microscopic model, the real part of optical model was taken as a Sao Paulo potential whereas the imaginary part was taken as Woods Saxon. The present analysis was performed using FRESCO **(Thompson, 2006)** with the parameters of the imaginary surface part. In the OM calculations, the Coulomb radius r_c=1.3 fm was taken. To obtain the best fit of the calculations with the experimental data, the normalization factor N_r and the imaginary surface potential parameters (W_s and a_s) must be adjusted where r_s= 1.292 fm was fixed. In the case of SM calculations (red lines), the N_r was in the range of 0.9 - 1.1. The reaction cross-section σ_R has been calculated using FRESCO. The volume integral of the imaginary part, J_w, has been calculated through the phenomenological equation **(Ali et al., 2018):**

$$\frac{J w_s}{A} = \frac{4\pi}{A}\int_0^\infty w_s(r) r^2 dr = \frac{4\pi}{3A} r_s{}^3 \left[1 + \left(\frac{\pi a_s}{R_s}\right)^2\right] \quad (9)$$

Table (1): Double folding of alpha elastically scattered by ^{6}Li using fresco code

Semi-microscopic parameters					
E(MeV)	**N_r**	**W_s(MeV)**	**a_s(fm)**	**Jw(MeV.fm^3)**	**σ_r(mb)**
29.4	0.9	15.0	0.62	59.52257	788.95
50.5	1.1	16.0	0.55	57.66086	686.17
59.0	0.9	17.0	0.50	57.29398	601.22
104.0	0.9	10.0	0.90	58.61639	784.24
166.0	1.0	20.0	0.60	77.19235	569.84
Full microscopic parameters					
E(MeV)	**N_R**	**N_i**	**σ_r(mb)**		
29.4	1.1	0.30	804.45		
50.5	1.2	0.35	729.45		
59.0	1.0	0.35	672.72		
104.0	0.9	0.50	611.60		
166.0	0.8	0.50	518.04		

Alpha elastically scattered by ^{7}Li

The study of the ^{7}Li nucleus is of particular interest because it is an isotope of ^{6}Li and contains clusters that can be classified as ^{2}H+^{5}He or t+^{4}He **(Shrivastava et al., 2013; Beck et al., 1981; Amar et al., 2021)**. The analysis of alpha elastically scattered by ^{7}Li has been done at energies (26.0, 29.4, 50.5, and 65.0 MeV) as shown in Fig. (2). The angular distributions were analyzed using microscopic and semi-microscopic models. The imaginary potential parameters are listed in Table (2) where r_s =1.34 fm **(Perey et al., 1976)** is fixed. The double-folded potential is calculated using the normalization factor, and the result is compared to experimental data until the calculated potential and the experimental data match as much as possible, the normalization factor's value is changed iteratively. The calculated cross-section σ_r decreased with the energy increase also the behavior of the volume integral J_w depending on energy increases up to 10-20 MeV per nucleon. The second fitting represented the full microscopic (FM) potential, with the normalization factors N_i and N_R presented in Table (2). It was observed that the FM analysis is better than the semi-microscopic analysis, especially at higher energies where the maximum value of N_R was obtained at E_d = 65.0 MeV.

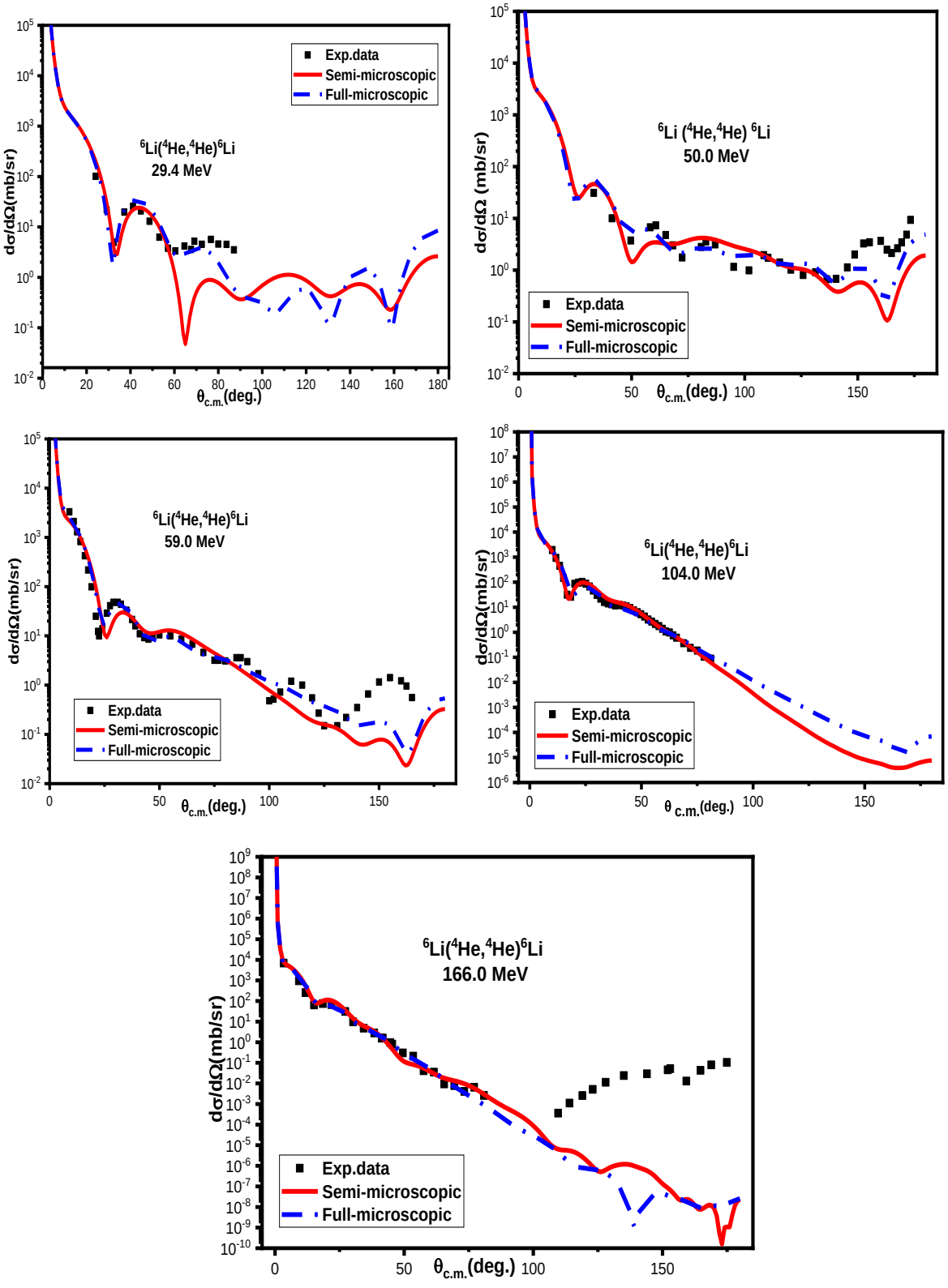

Fig. (1): Alpha elastically scattered by ^{6}Li at 29.4 MeV**(Matsuki, 1968),** 50.5 MeV**(Bragin et al., 1986),** 59.0 MeV**(Foroughi, et al., 1979),** 104.0 MeV **(Hauser et al., 1969),** and 166.0 MeV**(Bachelier et al., 1972)** where the squares represent the experimental data, solid lines represent semi-microscopic model and dash-dot lines represent full microscopic model

Table (2): Double folding of alpha elastically scattered by ^{7}Li using fresco code

Semi-microscopic parameters					
E(MeV)	**N_r**	**W_s(MeV)**	**a_s(fm)**	**J_w(MeV.fm^3)**	**σ_r(mb)**
26.0	1.2	8.0	0.8	39.53313	935.10
29.4	1.1	7.0	0.9	39.09497	986.26
50.5	1.0	17.0	0.5	58.91707	670.65
65.0	1.2	13.0	0.75	60.42851	848.03
Full microscopic parameters					
E(MeV)	**N_R**	**N_i**		**σ_r(mb)**	
26.0	1.1	0.2		789.25	
29.4	1.2	0.4		829.86	
50.5	1.2	0.4		734.18	
65.0	1.2	0.5		718.10	

Alpha elastically scattered by ^{9}Be

The comparison between the experimental data and the theoretical predictions for ^{4}He elastically scattered on ^{9}Be at energies (40.0, 45.0, 48.0, 50.0, 63.0, 65.0 and 90.0 MeV) are shown in Fig. (3) based on the potential parameters, which are listed in Table (3) where r_s=1.306 fm. To obtain a fit of the calculations with the experimental data, the N_r and the imaginary potential parameters must be adjusted. These parameters were changed freely until the best fit was obtained. The N_r factor was in the range of 0.9 - 1.2. At 45.0 MeV, the calculated reaction cross-section gives its maximum value while the J_w gives its minimum value. In the full microscopic method, the parameters N_i and N_R are varied freely until they obtain the best fit, as presented in Table (3). It should be noted that the FM analysis is satisfactory, especially at higher energies, as shown in Fig. (3).

Alpha elastically scattered by ^{11}B

The angular distributions for ^{4}He elastically scattered on ^{11}B at energies (29.0, 40.0, 48.7, 50.5, 54.1 and 65.0 MeV) is shown in Fig. (4). The potential depth of the surface imaginary part, diffuseness, and normalization factor (W_s, a_s and N_r) were varied freely until we had the best agreement between the theoretical calculations and experimental data, where r_s =1.34 fm was fixed, as presented in Table (4). Good analysis was obtained at alpha elastically scattered on ^{11}B in two models. The calculated reaction cross-section decreased with energy increased. It was observed that the FM analysis is better than the semi-microscopic analysis, especially at higher energies. The imaginary part of the FM model depends on nucleon-nucleon interaction through a folded model.

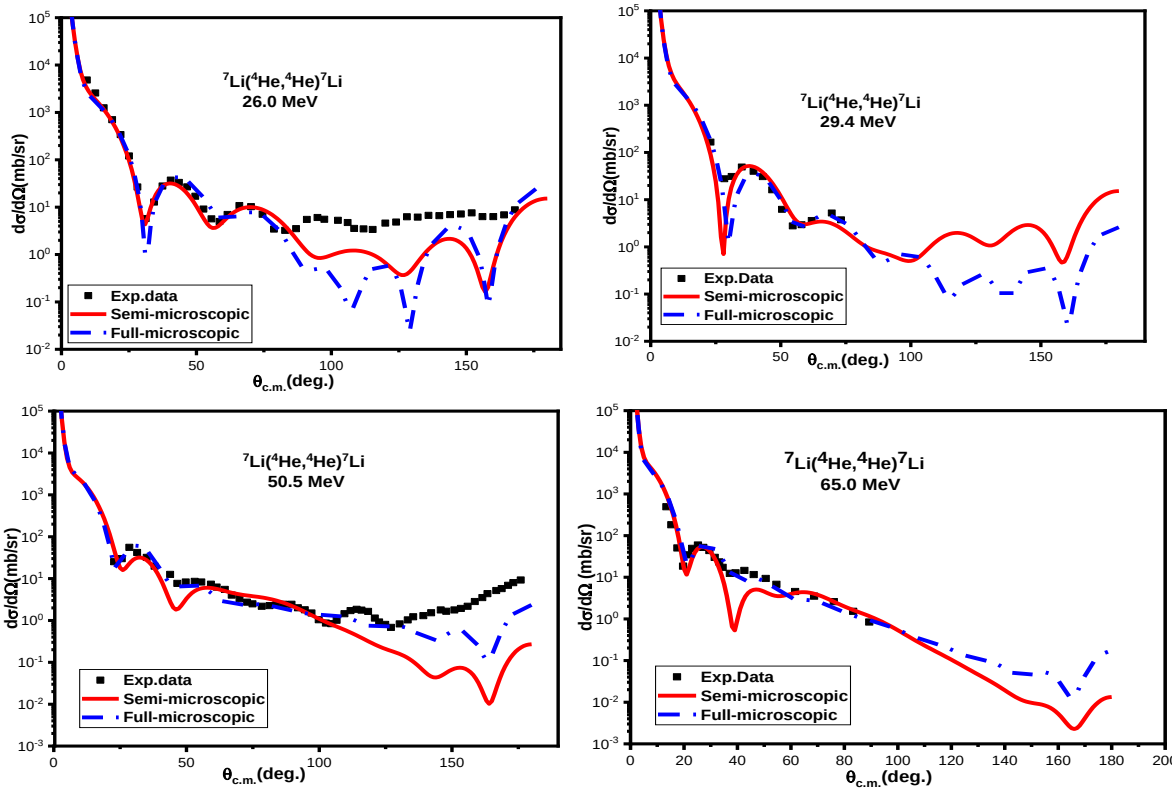

Fig. (2): Alpha elastically scattered by ^{7}Li 26.0 MeV **(Bingham et al., 1971)**, 29.4 MeV(**Matsuki, 1968**) ,50.5 MeV**(Burtebaev et al., 1996)** and 65.0 MeV (**Hamada et al.,** 1994) where the squares represent the experimental data, solid lines represent semi-microscopic model and dash - dot lines represent full microscopic model

Table (3): Double folding of alpha elastically scattered by ^{9}Be using fresco code

Semi-microscopic parameters					
E(MeV)	**Nr**	**W_s (MeV)**	**a_s (fm)**	**J_w (MeV.fm^3)**	**σ_r (mb)**
40.0	1.2	15.0	0.7	57.91358	944.88
45.0	1.2	10.0	0.6	34.5546	1011.57
48.0	1.0	16.0	0.6	55.28737	807.89
50.0	0.9	16.0	0.58	54.1097	772.24
63.0	0.9	16.0	0.58	54.1097	740.11
65.0	0.9	18.0	0.56	59.59346	733.57
90.0	1.1	19.0	0.7	73.3572	867.98

Full microscopic parameters			
E(MeV)	**N_R**	**Ni**	**σ_R(mb)**
40.0	0.9	0.3	770.78
45.0	0.9	0.3	750.45
48.0	1.1	0.3	768.34
50.0	1.1	0.35	778.26
63.0	1.1	0.45	767.77
65.0	0.9	0.5	776.67
90.0	1.1	0.35	662.24

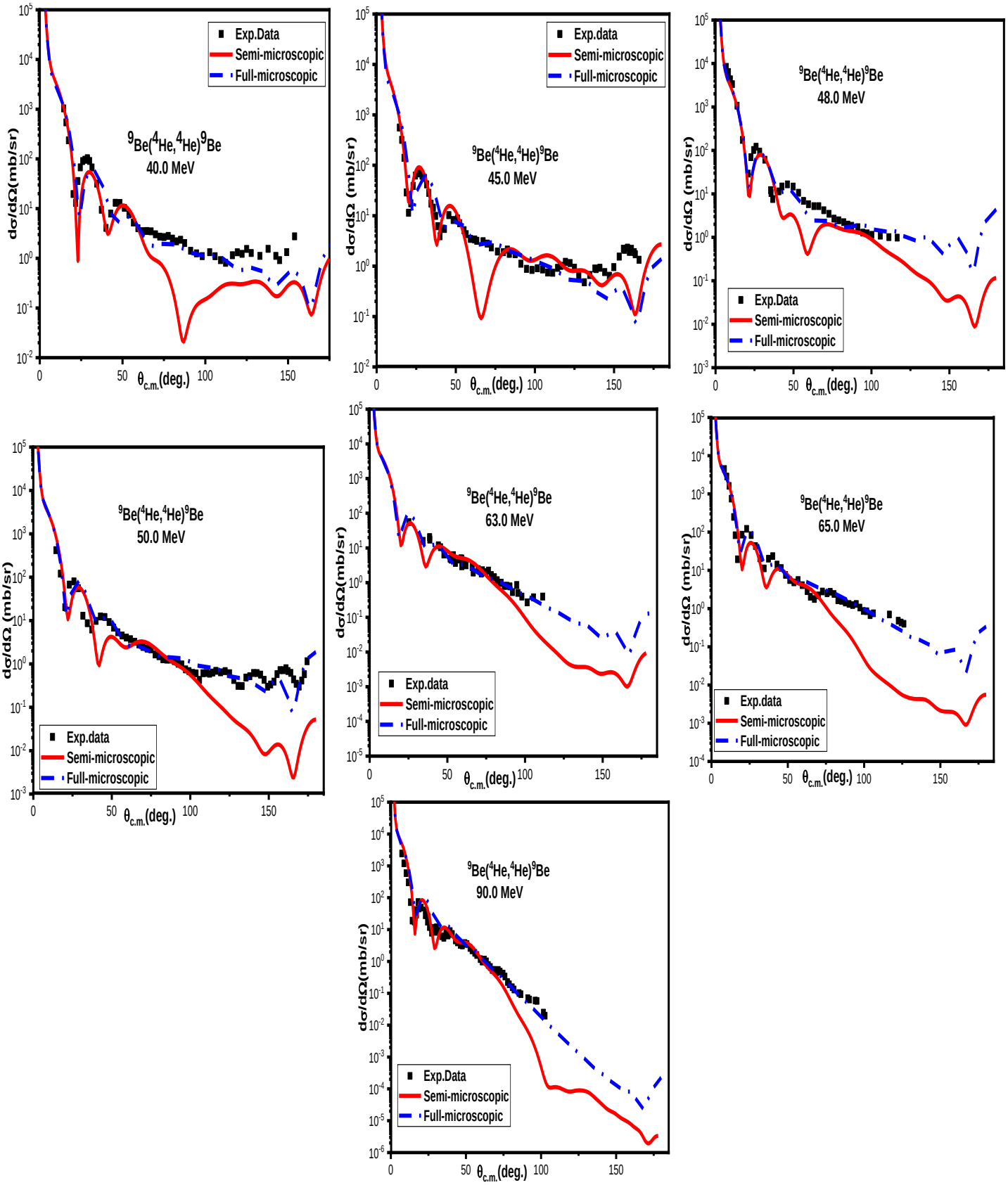

Fig.(3): Alpha elastically scattered by ^{9}Be at 40.0 MeV**(N.Burtebaev, 2002)**, 45.0 MeV**(N.Burtebaev, 2002)**, 48.0 MeV**(Summers-Gill, 1958)**, 50.0 MeV**(N.Burtebaev, 2002)**, 63.0 MeV**(Lukyanov et al., 2014)**, 65.0 MeV**(Roy et al., 1995)** and 90.0 MeV**(Demyanova et al., 2015)** where the squares represent the experimental data, solid lines represent semi-microscopic model and dash - dot lines represent full microscopic model

Table (4): Double folding of alpha elastically scattered on ^{11}B using fresco code

Semi-microscopic parameters					
E(MeV)	**N_r**	**W_s(MeV)**	**a_s(fm)**	**J_w(MeV.fm^3)**	**σ_r(mb)**
29.0	1.1	12.0	0.7	46.6979	1002.16
40.0	1.1	14.0	0.5	45.07363	808.82
48.7	1.2	17.0	0.5	54.73226	812.98
50.5	1.2	17.0	0.5	54.73226	807.47
54.1	1.2	17.0	0.5	54.73226	796.91
65.0	0.9	13.0	0.6	45.85777	792.51
Full microscopic parameters					
E(MeV)	**N_R**		**N_i**		**σ_r(mb)**
29.0	1.1		0.4		925.50
40.0	1.2		0.25		857.33
48.7	1.1		0.3		823.05
50.5	1.1		0.3		816.42
54.1	1.1		0.3		803.39
65.0	1.2		0.3		811.06

It also considers the relative speed between levels and the speed of light to overcome the Pauli effect through SPP. This potential gave good results at alpha particle energies around 50 MeV, approximately with all nuclei. At higher energy, the fitting is good for forward angles only. The relations between J_w, σ_r, N_r, W_s and a_s for the $\alpha+^{6,7}Li$, $\alpha+^{9}Be$, and $\alpha+^{11}B$ systems and alpha energy, are shown in Fig. (5). The behavior of the volume integral J_w depending on energy increases up to 10-20 MeV/ nucleon as shown in Fig. (5). The extracted normalization factors from the SPP potential are almost equal to unity. The cross-section decreases with increasing energy.

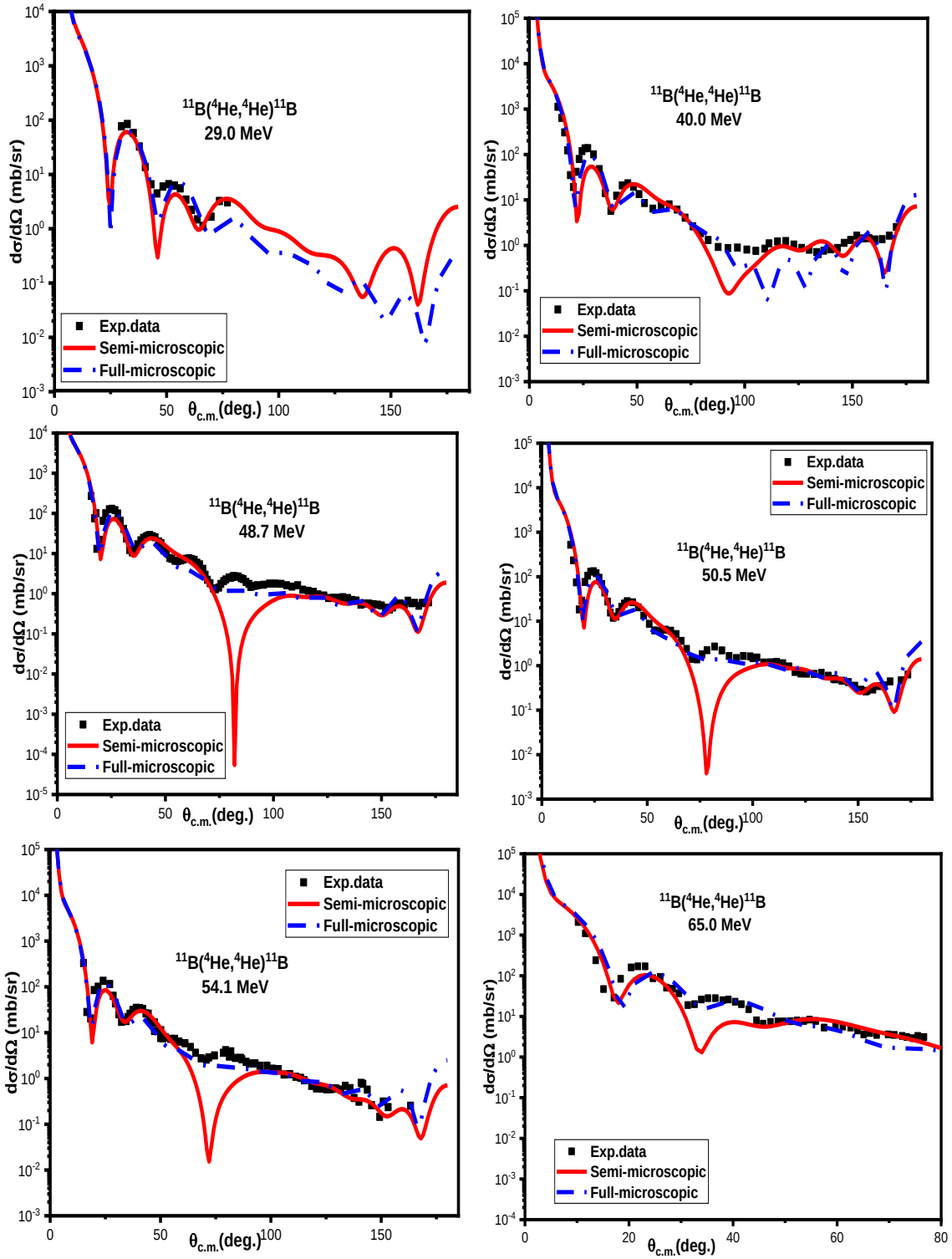

Fig. (4): Alpha elastically scattered by ^{11}B 29.0 MeV**(Burtebayev et al. 2018)**, 40.0 MeV**(Burtebaev et al., 2008)**, 48.7 MeV**(Abele et al., 1987),** 50.5 MeV**(Burtebaev et al., 2005)**, 54.1 MeV**(Abele et al., 1987)** and 65.0MeV**(Danilov et al., 2015)** where the squares represent the experimental data, solid lines represent semi-microscopic model and dash - dot lines represent full microscopic model

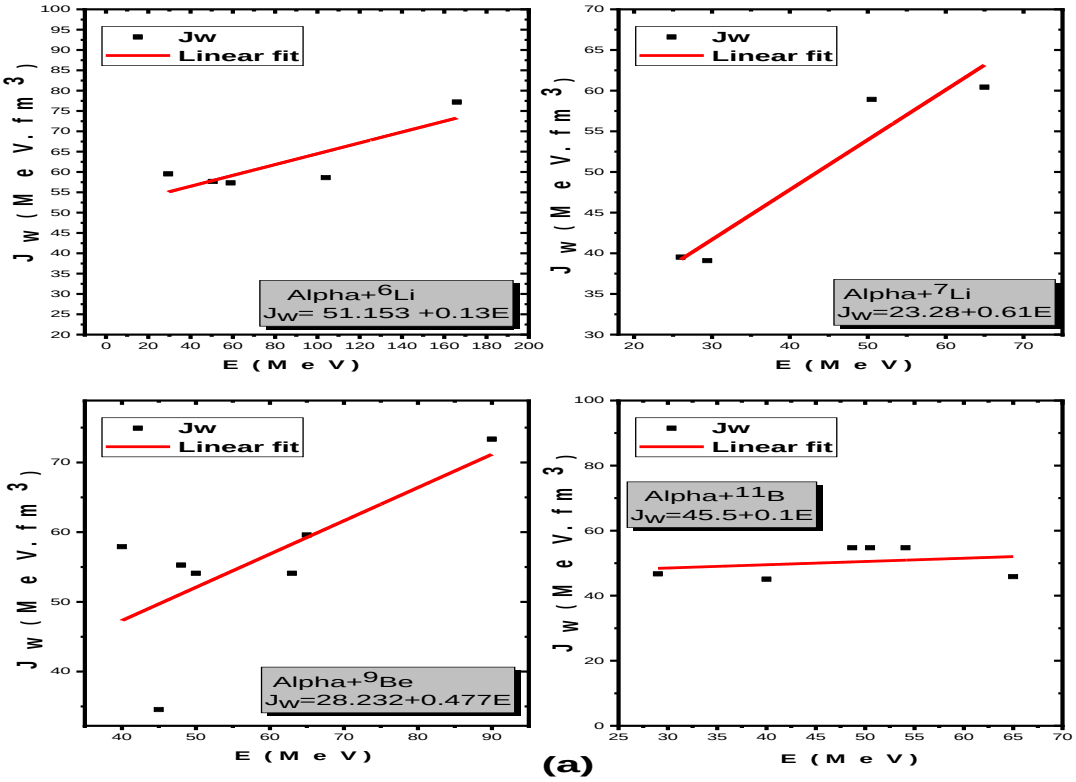
Jw
Linear fit
Alpha+6Li
Jw= 51.153 +0.13E
Alpha+7Li
Jw=23.28+0.61E
Alpha+9Be
Jw=28.232+0.477E
Alpha+11B
Jw=45.5+0.1E
J w (M e V. f m 3)
E (M e V)

(a)

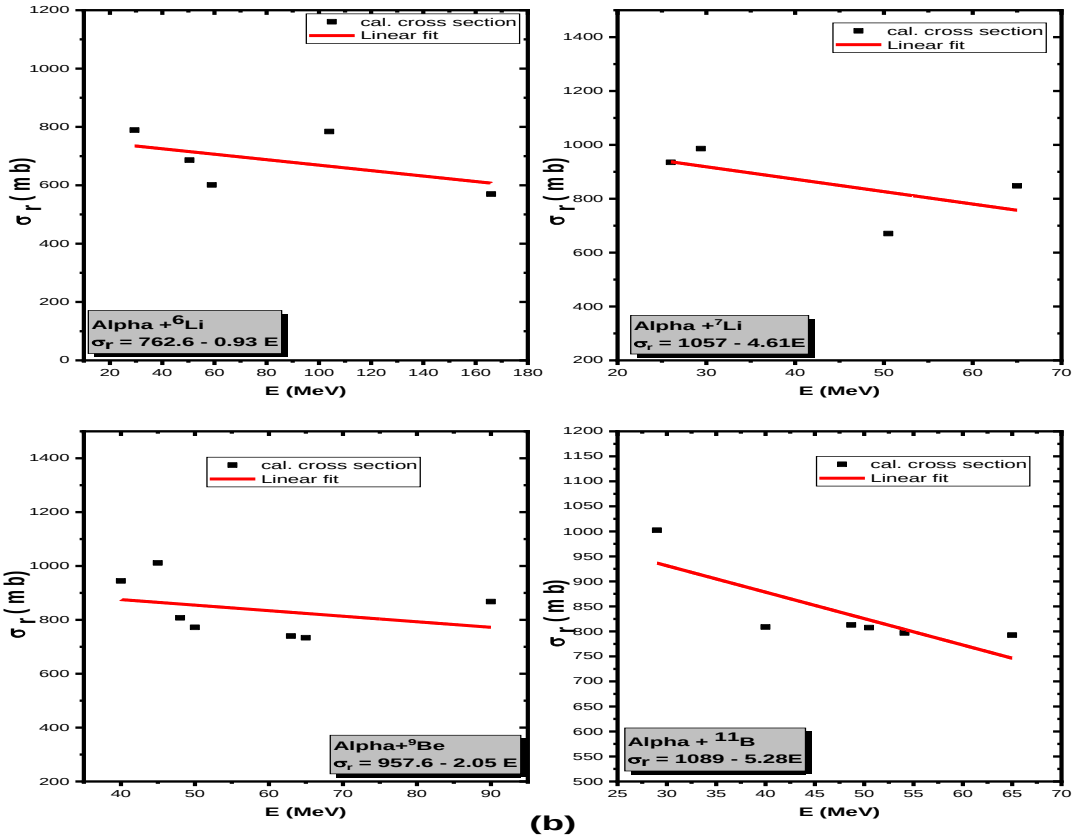
cal. cross section
Linear fit
Alpha +6Li
σr = 762.6 - 0.93 E
Alpha +7Li
σr = 1057 - 4.61E
Alpha+9Be
σr = 957.6 - 2.05 E
Alpha + 11B
σr = 1089 - 5.28E
σr(mb)
E (MeV)

(b)

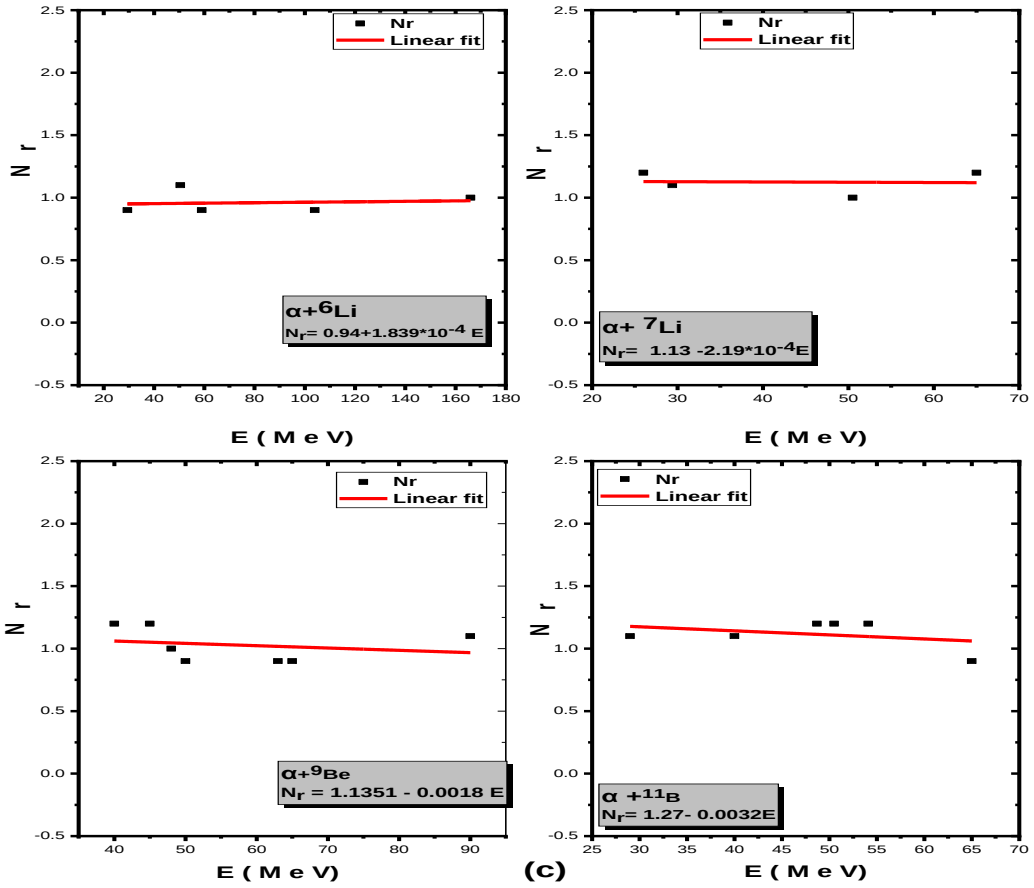
Nr
Linear fit
α+6Li
Nr= 0.94+1.839*10-4 E
α+ 7Li
Nr= 1.13 -2.19*10-4E
α+9Be
Nr = 1.1351 - 0.0018 E
α +11B
Nr= 1.27- 0.0032E
N r
E (M e V)

(c)

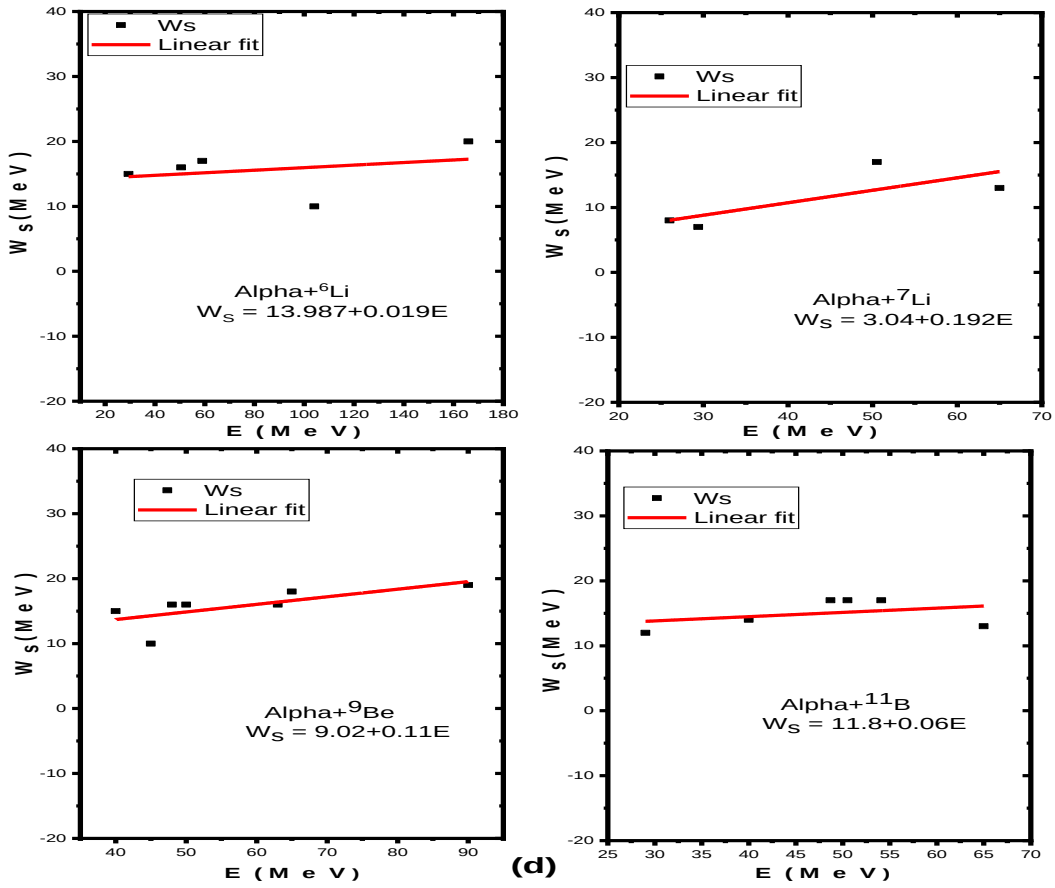
Ws
Linear fit
Alpha+6Li
Ws = 13.987+0.019E
Alpha+7Li
Ws = 3.04+0.192E
Alpha+9Be
Ws = 9.02+0.11E
Alpha+11B
Ws = 11.8+0.06E
Ws(MeV)
E (M e V)

(d)

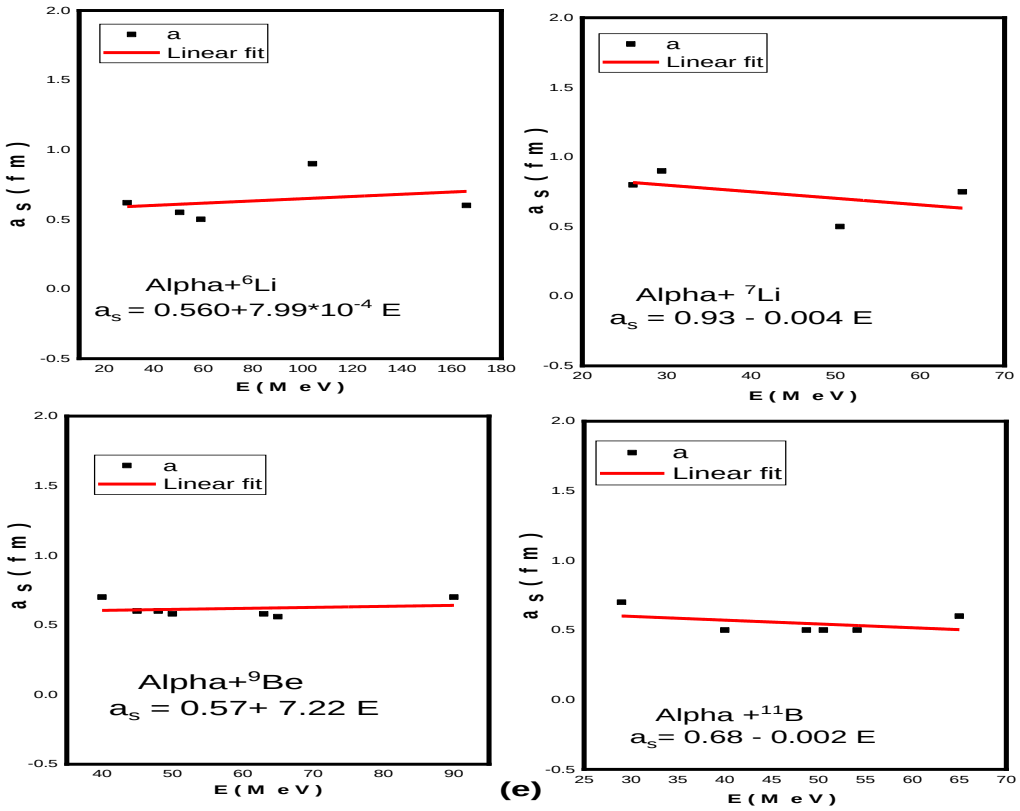

Fig. (5): The behavior of the optical potential parameters J_W(a), σ_r (b), N_R (c), W_S (d) and a_s (e), for $\alpha+^{6,7}$Li, $\alpha+^{9}$Be and $\alpha+^{11}$B systems

Conclusions

The double folding model was used to analyze the considered data semi-microscopically and full-microscopically. The Woods-Saxon form was used for the imaginary part of the SM model. All systems under examination have extracted normalization factors from the SPP potential that are almost equal to unity, indicating that the SPP potential might reasonably reproduce the experimental data. The Normalization factor exhibited an energy-dependent behavior for the systems. The semi-microscopic analysis is still valid to reproduce the differential cross-section at the forward angles. The Full microscopic analysis could reproduce the differential cross-section at forward and intermediate angles, where the analysis of the back-ward angles ($\theta > 120^{\circ}$) needs the transfer mechanisms. The Full microscopic analysis in our study is considered a good choice for studying nuclear reactions because we took into consideration the density distribution for both the incident and target nuclei and the local relative velocity between interactive nuclei in both the real and imaginary parts.

References

Abele, H., H. J. Hauser, A. Körber, W. Leitner, R. Neu, H. Plappert, T. Rohwer, et al. 1987. "Measurement and Folding-Potential Analysis of the Elastic α-Scattering on Light Nuclei." *Zeitschrift Für Physik A At. Nucl.* 326 (4): 373–81. https://doi.org/10.1007/BF01289540.

Ali, Fatimah Fadhil Abd, and Mahdi Hadi Jasim. 2018. "The Real and Imaginary Volume Integrals in Spherical-Statistical Optical Potential of Neutron Scattering from ^{56}Fe Nuclei." *Iraqi J. Sci.*, 59 (4): 2211–16. https://doi.org/10.24996/IJS.2018.59.4C.7.

Alvarez, M. A.G., L. C. Chamon, M. S. Hussein, D. Pereira, L. R. Gasques, E. S. Rossi, and C. P. Silva. 2003. "A Parameter-Free Optical Potential for the Heavy-Ion Elastic Scattering Process." *Nucl. Phys. A* 723 (1–2): 93–103. https://doi.org/10.1016/S0375-9474(03)01158-8.

Amar, A. 2022. "Analysis of Alpha Elastically Scattered by Light Nuclei Applying Different Models." *Inter. J. Mod Phys. E* 31 (2): 2250011. https://doi.org/10.1142/S0218301322500112.

Amar, A., and Awad A. Ibraheem. 2021. "Elastic Scattering of Light Nuclei by Deuterons with Different Models." *Inter. J. Mod. Phys. E* 30 (10). https://doi.org/10.1142/S0218301321500907.

Amar, A, Ashraf M El Mhlawy, A H Amer, and A R El Sayed. 2022. "Investigation the Elastic Scattering of Isobar Nuclei ^{6}Li and ^{6}He by ^{12}C Using Different Nuclear Potentials 7." *Inter. J. Mod. Phys. E* 31 (3). https://doi.org/10.1142/S0218301322500264.

Amer, A.H., Y.E. Penionzhkevich, A.A. Ibraheem, and Sh. Hamada. 2020. "Comparison between the Elastic Scattering of ^{12}C(d,d)^{12}C and ^{12}C(^{6}He, ^{6}He)^{12}C Using Different Nuclear Potentials." *Inter. J. Mod. Phys. E*, 29. https://doi.org/10.1142/S0218301320500086X.

Amer, Ahmed H, A Amar, Sh Hamada, I. I. Bondouk, and F. A. El-Hussiny. 2016. "Optical and Double Folding Model Analysis for Alpha Particles Elastically Scattered from ^{9}Be and ^{11}B Nuclei at Different Energies." *Inter. Chem, Molecu., Nucl., Mater. and Metallurg. Eng.* 10 (2): 161–66.

Amer, Ahmed Hammad, and Yu E. Penionzhkevich. 2021. "Elastic Scattering Analysis of Isobar Nuclei A = 6 Projectiles on ^{12}C Using Different Models of Optical Potential." *Nucl. Phys. A* 1015: 122300. https://doi.org/10.1016/j.nuclphysa.2021.122300.

Bachelier, D., M. Bernas, J. L. Boyard, and et al. 1972. *Nucl. Phys* 195: 361.

Beck, R, R Krivec, and M. V. Mihailovie. 1981. "The Three-Cluster Structures in ^{6}Li,^{7}Li, ^{9}Be and ^{11}B." *Nucl. Phys. A* A363: 365–80. https://doi.org/10.1016/0375-9474(81)90263-3.

Bingham, H. G., K. W. Kemper, and N. R. Fletcher. 1971. *Nucl. Phys. A* 175: 374.

Burtebaev, N., M. K. Baktybaev, B. A. Duisebaev, R. J. Peterson, and S. B. Sakuta. 2005. "Scattering of α Particles on ^{11}B Nuclei at Energies 40 and 50 MeV." *Phys. At. Nucl.*68 (8): 1303–13. https://doi.org/10.1134/1.2011493.

Burtebaev,N., Baktybaev, M.K, Duisebaev B.A., Peterson R. J., and Sakuta S. B. 2005. "Scattering of α Particles on ^{11}B Nuclei at Energies 40 and 50 MeV." *Phys. At. Nucl.* 68 (8): 1303–13. https://doi.org/10.1134/1.2011493.

Burtebaev, N., A. D. Duisebaev, B. A. Duisebaev, G. N. Ivanov, and S. B. Sakuta. 1996. "Elastic and Inelastic Scattering of 50-MeV α Particles by ^{6}Li and ^{7}Li Nuclei: The Role of Exchange Effects in Anomalous Scattering at Large Angles." *Phys. At. Nucl.* 59 (1): 29–37.

Burtebayev, N., D. M. Janseitov, Zh Kerimkulov, D. Alimov, M. Nassurlla, D. S. Valiolda, B. Urazbekov, A. S. Demyanova, V. Starastsin, and A. N. Danilov. 2020. "Elastic Scattering of Alpha Particles from ^{9}Be in the Framework of Optical Model." *J. Phys.: Conf. Series* 1555 (1): 1–7. https://doi.org/10.1088/1742-6596/1555/1/012032.

Burtebayev, N., Zh Kerimkulov, M. Bakhtybayev, Sh Hamada, Y. Mukhamejanov, M. Nassurlla, D. Alimov, A. Morzabayev, D. Janseitov, and W. Trzaska. 2018. "Investigation of the Elastic and Inelastic Scattering of ^{4}He from ^{11}B in the Energy Range 29-50.5 MeV." *J. Phys: Conf. Series* 940 (1): 012034. https://doi.org/10.1088/1742-6596/940/1/012034.

Chamon, L. C. 2007. "The São Paulo Potential." *Nucl. Phys. A* 787 (1-4 SPEC. ISS.): 198–205. https://doi.org/10.1016/j.nuclphysa.2006.12.032.

Chamon, L. C. 2013. SPOMC3 Computational Code, 05315 970.

Chamon, L. C., Carlson, B. V., Gasques, L. R., Pereira, D., De Conti, C., Alvarez, M. A.G., Hussein, M. S., Cândido Ribeiro, M. A., Rossi, E. S., and Silva, C. P. 2002. "Toward a Global Description of the Nucleus-Nucleus Interaction." *Phys. R. C - Nucl. Phys.* 66 (1): 146101–13. https://doi.org/10.1103/PhysRevC.66.014610.

Danilov, A. N., Demyanova, A. S. Dmitriev, S. V., Ogloblin, A. A., Belyaeva, T. L., Goncharov, S. A., Gurov, Yu. B., et al. 2015. "Study of Elastic and Inelastic ^{11} B +α Scattering and Search for Cluster States of Enlarged Radius in ^{11}B." *Phys. At. Nucl.* 78 (6): 777–93. https://doi.org/10.1134/S1063778815060071.

Demyanova, A. S., A. A. Ogloblin, A. N. Danilov, S. V. Dmitriev, V. I. Starostin, S. A. Goncharov, T. L. Belyaeva, et al. 2015. "Neutron Halo in the Exotic First Excited State of ^{9}Be." *ZEP* 102 (7): 413–16. https://doi.org/10.1134/S0021364015190030.

Foroughi, F., E. Bovet, and Ch Nussbaum. 1979. "Elastic and Inelastic Scattering of Alpha Particles from ^{6}Li at 59 MeV." *J. Phys. G: Nucl. Phys.* 5 (12): 1731–40. https://doi.org/10.1088/0305-4616/5/12/012.

Gasques, L. R., L. C. Chamon, D. Pereira, M. A.G. Alvarez, E. S. Rossi, C. P. Silva, G. P.A. Nobre, and B. V. Carlson. 2003. "Systematical Study of the Optical Potential for Systems like A+ ^{58}Ni from Sub-Barrier Data Analyses." *Phys. R. C - Nucl. Phys.* 67 (6): 676031–34. https://doi.org/10.1103/physrevc.67.067603.

Gómez Camacho, A., P. R.S. Gomes, and J. Lubian. 2011. "Woods-Saxon and

São Paulo Optical Model Calculations of the Threshold Anomaly of the ^{6,7}Li+^{28}Si Systems near Coulomb Barrier Energies." *J. Phys.: Conf. Series* 322 (1). https://doi.org/10.1088/1742-6596/322/1/012008.

Hamada, S., M. Yasue, S. Kubono, M.H. Tanaka, and R.J. Peterson. 1994. "Cluster Structures in ^{10}Be from the ^{7}Li(Alpha, p)^{10}Be Reaction." *Phys. R. C* 49 (6): 3192.

Hamada, Sh, and Awad A. Ibraheem. 2023. "Phenomenological and Microscopic Analysis for the ^{7}Li + ^{12}C System." *Nucl. Phys. A* 1030: 122590. https://doi.org/10.1016/j.nuclphysa.2022.122590.

Hauser, G., R. Lohken, H. Rebel, and Et Al. 1969. *Nucl. Phys. A* 128: 81.

Ibraheem, Awad A. 2016. "Analysis of Deuteron-Nucleus Scattering Using Sao Paulo Potential." *Braz. J. Phys.* 46 (6): 746–53. https://doi.org/10.1007/s13538-016-0453-0.

Ibraheem, Awad A., M. El-Azab Farid, Eman Abd El-Rahman, Zakaria M.M. Mahmoud, and Sherif R. Mokhtar. 2020. "Different Folding Models for ^{6}Li+ ^{28}Si Elastic Scattering." *Inter. J. Mod. Phys. E* 29 (9). https://doi.org/10.1142/S0218301320500755.

Lukyanov, S. M., A. S. Denikin, E. I. Voskoboynik, S. V. Khlebnikov, M. N. Harakeh, V. A. Maslov, Yu E. Penionzhkevich, et al. 2014. "Study of Internal Structures of ^{9,10}Be and ^{10}B in Scattering of ^{4}He from ^{9}Be." *J. Phys. G: Nucl. Particle Physics* 41 (3): 035102. https://doi.org/10.1088/0954-3899/41/3/035102.

Matsuki, Seishi. 1968. "Disintegration of ^{7}Li and ^{6}Li by 29.4 MeV Alpha-Particles." *J. Phys. Soci. Jap.* 24 (6): 1203–23. https://doi.org/10.1143/JPSJ.24.1203.

N.Burtebaev. 2002. "Investigation of Mechanism of Alpha Particles Elastic Scattering on ^{9}Be Nucleus." *VAT/Y* 137: 1–2.

Perey, C. M., and F. G. Perey. 1976. "Compilation of Phenomenological Optical-Model Parameters 1954-1975." *At. Data Nucl. Data Tables* 17 (6): 1–101. https://doi.org/10.1016/S0092-640X(72)80015-9.

Qaim, Syed M., Ingo Spahn, Bernhard Scholten, and Bernd Neumaier. 2016. "Uses of Alpha Particles, Especially in Nuclear Reaction Studies and Medical Radionuclide Production." *Radiochimica Acta* 104 (9): 601–24. https://doi.org/10.1515/ract-2015-2566.

Roy, Subinit, J. M. Chatterjee, H. Majumdar, S. K. Datta, S. R. Banerjee, and S. N. Chintalapudi. 1995. "Coupled Channel Folding Model Description of Scattering from ^{9}Be." *Phys. R. C* 52 (3): 1524–31. https://doi.org/10.1103/PhysRevC.52.1524.

Saad, S. S. 1995. "Folding-Potential Analysis of the Elastic ^{4}He-Scattering on ^{6}Li." *Applied Radiation and Isotopes* 46 (1): 23–27. https://doi.org/10.1016/0969-8043(94)00088-H.

Shrivastava, A., A. Navin, A. Diaz-Torres, V. Nanal, K. Ramachandran, M. Rejmund, S. Bhattacharyya, et al. 2013. "Role of the Cluster Structure of ^{7}Li in the Dynamics of Fragment Capture." *Phys. Letters, Sec. B: Nucl., Elementary Particle and High-Energy*

Thompson, I.J. 2006. "Fresco 2.0." *Department of Phys., University of Surrey, Guildford*.

V.N.Bragin, A.D.Dujsebaev N.T.Burtebaev, G.N.Ivanov, S.B.Sakuta, V.I.Chuev, and L.V.Chulkov. 1986. "Role of Exchange Effects in Elastic Scattering of Alpha Particles and of ^{3}He Ions by ^{6}Li Nuclei." *Yadernaya Fizika* 44: 312.

Phys. 718 (3): 931–36. https://doi.org/10.1016/j.physletb.2012.11.064.

Summers-Gill, Robert G. 1958. "Scattering of 12-Mev Protons, 24-Mev Deuterons, and 48-Mev Alpha Particles by Beryllium." *Phys. R.* 109 (5): 1591–1603. https://doi.org/10.1103/PhysRev.109.1591.

تشتت ألفا المرن بواسطة الأنوية الخفيفة باستخدام الطرق شبه المجهرية والمجهرية الكاملة

روان فرج ، أ.د. أحمد عمار ، أ.د. سلوى سعد

قسم الفيزياء – كلية العلوم- جامعة طنطا – طنطا – مصر

يهدف العمل الحالي إلى استخدام الطرق شبه المجهرية والمجهرية الكاملة لتحليل النتائج العملية للألفا المشتتة بشكل مرن على ^{6,7}Li، ^{9}Be، و^{11}B في نطاق الطاقات من ٢٦ إلى ١٦٦ MeV. في الطريقة شبه المجهرية تم استخدام جهد ساو باولو المزدوج (SPP) كجزء حقيقي من الجهد الضوئى في حين تم استخدام شكل وودز-ساكسون كجزء تخيلى وقد تم حساب الجزء الحقيقي من الجهد الضوئى عن طريق طي تفاعل النوكليون والنوكليون (NN) مع كثافة المادة النووية لكل من الجسم الساقط والهدف باستحدام برنامج SPOMC3. لقد وجدنا أن متغيرات النموذج الضوئى ومعاملات التصحيح لها تأثير على تفسير النتائج العملية. كما وجدنا أيضا أن التكامل الحجمى للجزء التخيلى من الجهد الضوئى ومقطع التفاعل يعتمدان على طاقة الأجسام الساقطة ولكن فى الطريقة المجهرية الكاملة تم استخدام جهد ساوباولو SPP كجزء حقيقى وتخيلى من الجهد الضوئى وهذا أعطى نتائج أفضل من الطريقة شبه المجهرية وذلك لأن كثافة المادة النووية لكل من الهدف والجسم الساقط وأيضا الجهد النووى للنيوكليونات أخذا فى الاعتبار.